A bioorthogonal chemistry approach to the study of biomolecules in their ultrastructural cellular context

Elsland, D.M. van

3

Electron Microscopy of Bioorthogonally-Labelled Biomolecules*

Introduction

Bioorthogonal chemistry is a powerful tool to image (sub)-populations of biomolecules in complex biological systems. Its mechanism relies on the introduction of a physiologically-inert tag into a biomolecule of interest that can be reacted with a detection moiety using a chemical reaction selective solely for this chemical moiety.[1] The small size of the chemical tag, which minimally interferes with cellular biochemistry and the broad scope of the labelling strategies make this method a valuable part of the biochemist's toolkit.[2, 3] It has proven especially powerful for the labelling of nongenetically-templated biomolecules such as glycans[4], lipids[5, 6], peptidoglycans[7, 8] and even active sub-populations of proteins using activity-based probes.[9, 10] Moreover, the approach is amenable to labelling biomolecules in a wide range of cell types and species spanning the prokaryotes, eukaryotes and metazoans.[11]

* Published as part of: Daphne M. van Elsland, Erik Bos, Wouter de Boer, Herman S. Overkleeft, Abraham J. Koster and Sander I. van Kasteren. *Chem. Sci*, **7**, 752-758 (2016). W.S. Jong and J. Luirink are kindly acknowledged for providing the HbpΔβ-cleav plasmid.

The most commonly used detection techniques for the imaging of bioorthogonal handles are the reaction of these moieties with biotin, FLAG tags, or with a fluorophore for direct visualisation using confocal fluorescence microcopy.[2] However, the main limitations of all these imaging approaches is the lack of resolution and the lack of information regarding the cellular environment in which these bioorthogonally-labelled molecules reside. Attempts to address this with super resolution microscopy have been reported[12], but this technique only provides the localisation information of the labelled molecule to very high accuracy but does not provide ultrastructural information of the cellular context of the handle.

Electron microscopy (EM) on the other hand, allows to map cellular ultrastructures at nanometer-scale resolution,[13] but the identification of specific biomolecules using conventional EM-approaches can be cumbersome.[14] Most readily the identification of biomolecules within EM imaged specimens is established upon colloidal gold labelling. Colloidal gold can be functionalised with macromolecules used in immunocytochemistry, such as protein A, antibodies, lectins or even polysaccharides.[15] It can be easily visualised with the electron microscope due to its electron-dense character and gives a punctate and precise labelling pattern. These features make them favourable for the localisation of biomolecules within structures studied at nanometer-scale resolution. Additionally, their particulate nature allows the labelling to be quantified with the possibility of estimating the amount of a particular protein molecule in a given structure.[15, 16]

Besides colloidal gold markers, which are directly visible in the EM, one can also decide to use fluorescent markers;[17] an approach known as CLEM (correlative light and electron microscopy). It combines the strengths of both light microscopy (LM) and EM imaging. For example, an image acquired with fluorescence microscopy (whereby fluorescently labelled biomolecules are identified) is overlaid on an EM image, which provides ultrastructural context to the fluorescent signal.[18] To date, CLEM has been used successfully to image GFP-fusion proteins, biomolecules labelled with immunofluorescence,[19, 20] or for the detection of small molecule fluorophores.[19-22]

These labelling techniques have, however, not been exploited to localise bioorthogonal groups in biological samples. One problem may be partial loss of the bioorthogonal functional groups during the (often harsh) conditions required for resin embedding of the samples (e.g. heating in presence of epoxide during Epon-embedding or exposure to radical polymerisation during Lowicryl-embedding).[23] This, combined with the fact that the yield of the bioorthogonal detection reaction must be very high and essentially background-free to allow detection of the label in ultrathin sections, may have prevented the application of this imaging modality to the detection of bioorthogonal functionalities in biological samples to date.

In this chapter the method development of EM compatible bioorthogonal labelling approaches are presented. These approaches build further on the Tokuyasu technique commonly used for on-section immuno-labelling[21, 24] which uses vitrification of cryoprotected, aldehyde-fixed samples and subsequent cryosectioning. The first method presented makes use of gold labelling, allowing the direct EM-visualisation of bioorthogonal groups in a biological sample. The second approach is a CLEM-based approach. This approach uses bioorthogonal fluorophore labelling and fluorescence microscopy prior to EM contrast enhancement and EM imaging of the same section. These methods were developed using the model bacterium *Escherichia coli* (*E. coli*). In this bacterium bioorthogonal azide handles[25, 26] can be readily incorporated by replacement of the methionine (Met) with azidohomoalanine (Aha) in the Met auxotrophic strain B834(DE3).[27, 28]

Results

Aha-incorporation in *E.coli* B834(DE3) was optimised with respect to cell viability and amount of incorporation. Culturing *E. coli* B834(DE3) for > 1 hour in the presence of 4 mM Aha (azido-*E. coli*) resulted in reduced outgrowth in comparison to cultures grown in the presence of Met (Figure 1). As well as showing reduced outgrowth, inclusion bodies were found to be formed at these time points (Figure 2), suggesting negative effects on protein folding upon prolonged exposure to Aha.[29] Labelling for 1 h in the presence of 4 mM Aha gave a robust signal throughout the *E. coli* proteome and showed minimal inhibition of viability (supported by[30]; Figure 3). These conditions (1 h, 4 mM Aha) were used for all further imaging studies.

Next it was tested whether the azido-*E. coli* B834(DE3) cells could be labelled with gold particles. Initial attempts aiming to directly conjugate gold particles to the bioorthogonal groups proved unsuccessful. But a labelling method based on a two-step strategy did prove fruitful: bioorthogonal copper-catalysed Huisgen cycloaddition (ccHc) was performed with a fluorophore,[31-33] followed by immunogold labelling against the fluorophore (Figure 4A). This two-step gold labelling strategy was tested on the surface of whole mount *E. coli* cells.

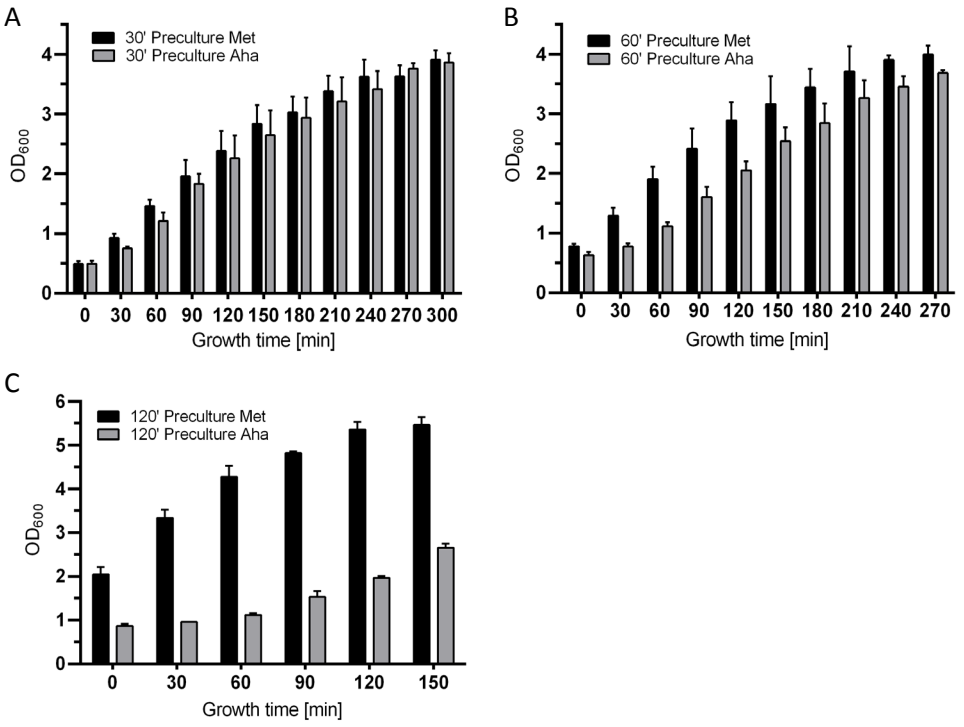

Figure 1: Outgrowth of *E. coli* B834(DE3) that were cultured in the presence of Aha (n=2): *E. coli* B834(DE3) cells were grown to an OD_{600} of 0.3-0.5. Cultures were then incubated with 4 mM Aha for either 30(A), 60(B) or 120 minutes (C). Cells were then collected and left to grow in LB medium. OD_{600} was measured at indicated time points. Cultures grown in the presence of Aha for t > 60 minutes showed severe effects on the outgrowth.

To ensure a high density of bioorthogonally labelled proteins on the surface of *E. coli*, *E. coli* B834(DE3) was transformed with the uncleavable autotransporter protein hemoglobin protease (Hbp).[34, 35] Upon incorporation of Aha in both the Hbp(Δβ-cleav) expressing and the Wild type (Wt) bacteria, the bioorthogonal gold labelling strategy resulted in a robust labelling of the *E. coli* surface. Surface

labelling of the Hbp(Δβ-cleav)-transformed *E. coli* was more pronounced compared to Wt *E. coli*, demonstrating the presence of bioorthogonally labelled Hbp(Δβ-cleav) (Figure 4B). Expression of the Hbp(Δβ-cleav) in the presence of 4 mM Aha was additionally confirmed with SDS-PAGE (Figure 5).

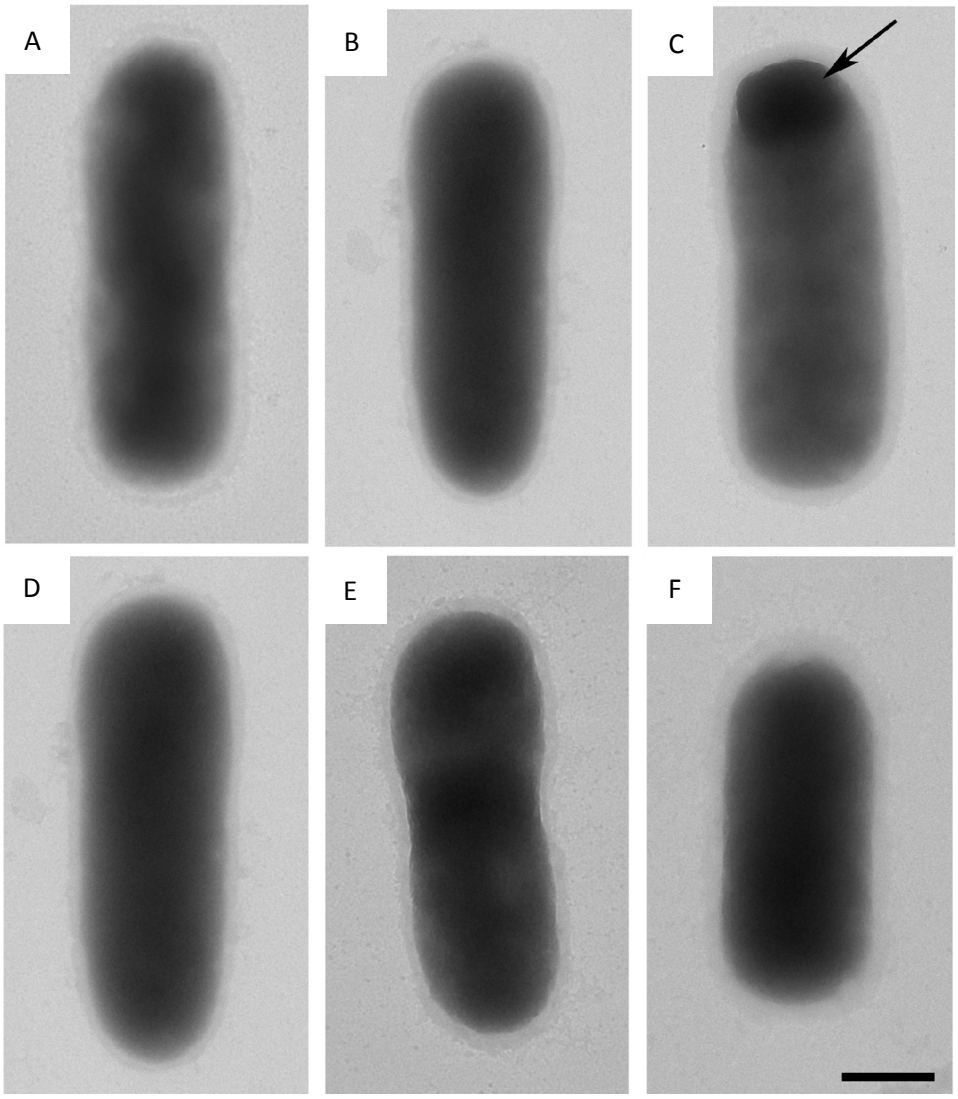

Figure 2: Inclusion body formation in *E. coli* B834(DE3) that were grown in the presence of Aha. *E. coli* B834(DE3) cells were grown to an OD_{600} of 0.3-0.5. Cultures were then incubated with 4 mM Aha (A-C) or 4 mM Met (D-F). After 30 (A, D), 60 (B, E) and 120 minutes (C, F) cells were harvested, fixed with 2% PFA and imaged with the electron microscope. Inclusion bodies were present in *E. coli* cells cultured for 120 minutes in the presence of 4 mM Aha (C). Inclusion body is indicated with an arrow. Scale bar 500 nm.

A

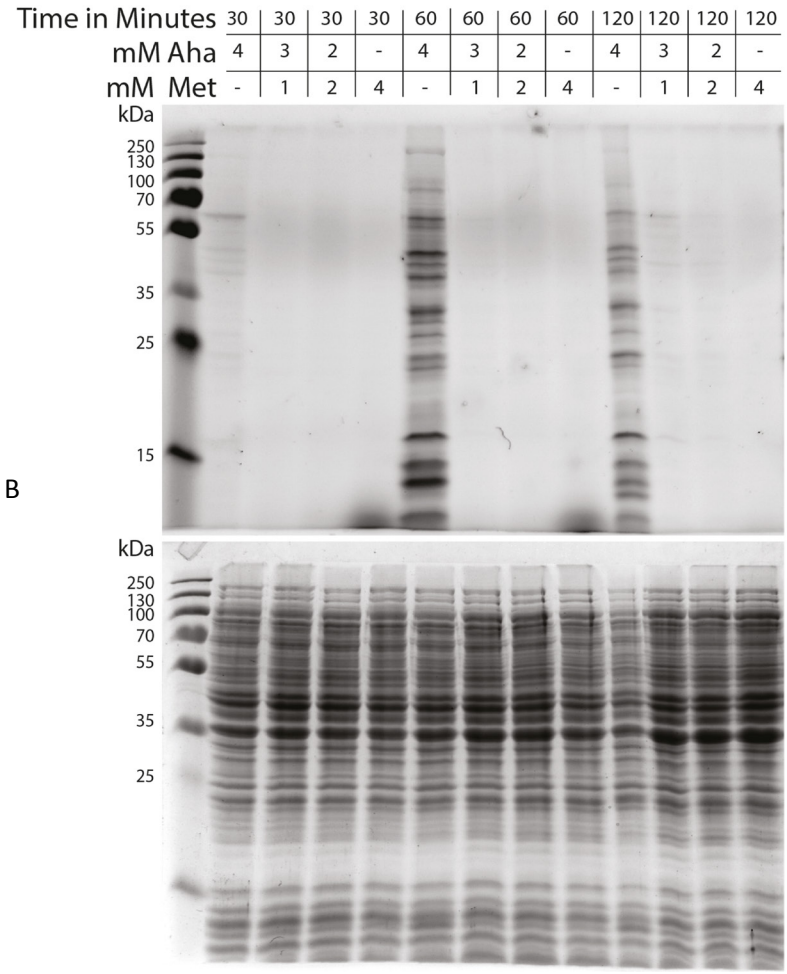

Figure 3: Aha incorporation in *E. coli* B834(DE3): (A) Fluorescence gel of AlexaFluor-488 alkyne-labelled *E. coli* cells grown in the presence of the indicated concentrations of Aha and Met. Maximal label incorporation was seen after 60 minutes in absence of Met and in presence of 4 mM Aha. (B) Coomassie-staining loading control shows relative amounts of total proteins per sample.

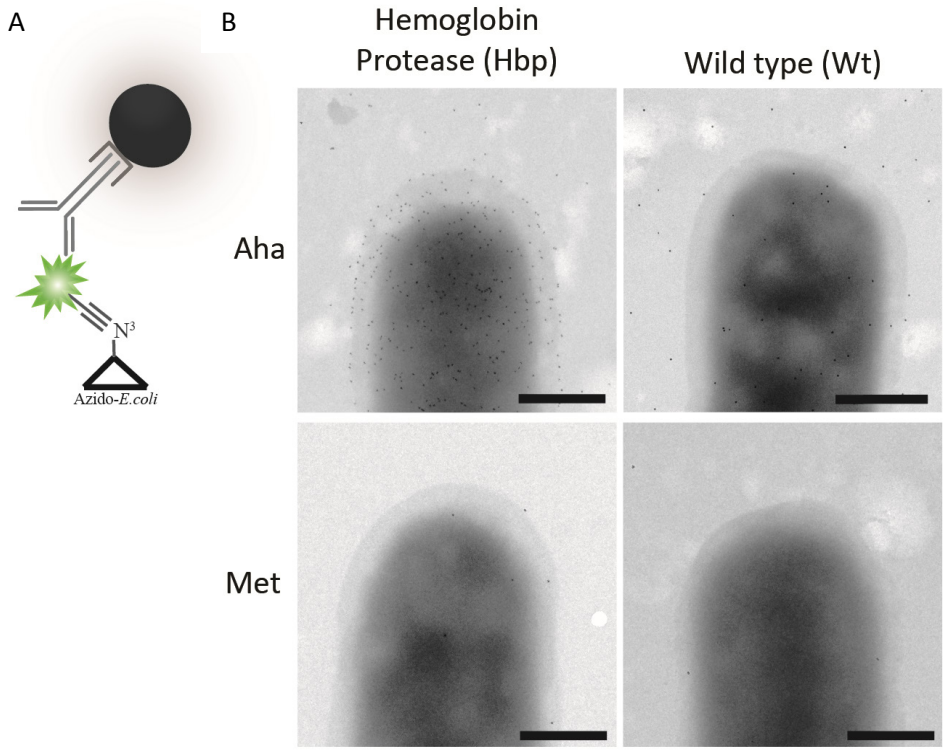

Figure 4: A) Schematic overview of bioorthogonal gold labelling strategy. Azido-*E. coli* B834(DE3) cells are surface-labelled with AlexaFluor-488 alkyne (green), after which gold particle labelling is performed using a rabbit anti-AlexaFluor-488 binding step. B) Bioorthogonal gold surface-labelling of Hbp (Δβ-cleav)-expressing and Wild type (Wt) *E. coli* B834(DE3) bacteria cultured in the presence of either 4 mM Aha or 4 mM Met. Scale bars 500 nm.

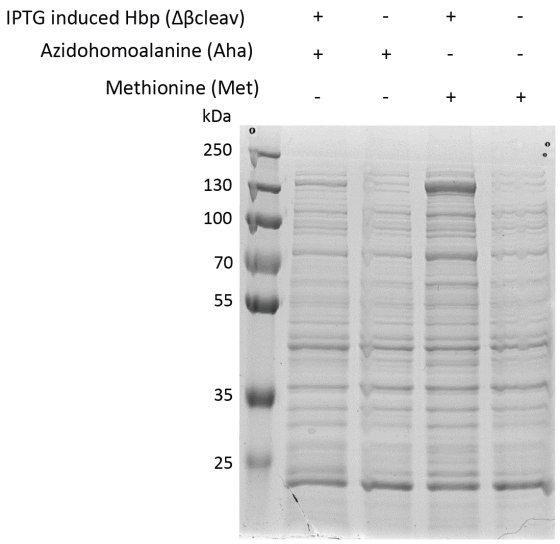

Figure 5: Coomassie-stained SDS-PAGE gel of *E. coli* B834(DE3) cells with/without Hbp(Δβ-cleav) expression and grown in the presence of either 4 mM Aha or 4 mM Met.

To ensure the analysis of bioorthogonal labelling on ultrastructures, it was next tested whether the bioorthogonal tagged *E. coli* B834(DE3) cells could be specifically gold-labelled after Tokuyasu sample preparation and cryosectioning.[36] To this end a mixture of the bioorthogonal tagged azido-*E. coli* cells and *E. coli* control cells (grown in the presence of Met) was subjected to Tokuyasu sample preparation. *E. coli* cells (Aha and Met treated) were fixed for 24h in 0.1 M phosphate buffer containing 2% paraformaldehyde (PFA). Labelling with the bioorthogonal gold labelling method shows that the azido-*E. coli* bacteria could be labelled and detected within a mixture with Met control cells (Figure 6). The ccHc reaction has sufficient signal-to-noise ratio for detection of azides even in ultrathin sections. Fixation of the bacteria with 2% PFA supplemented with 0.2% glutaraldehyde (GA) gave undesired background labelling, which is clearly visible on the Met treated control cells (Figure 7). This background was also present on whole mount *E. coli* cells upon fixation with 0.2% GA (Figure 7). All following fixations were therefore performed without GA.

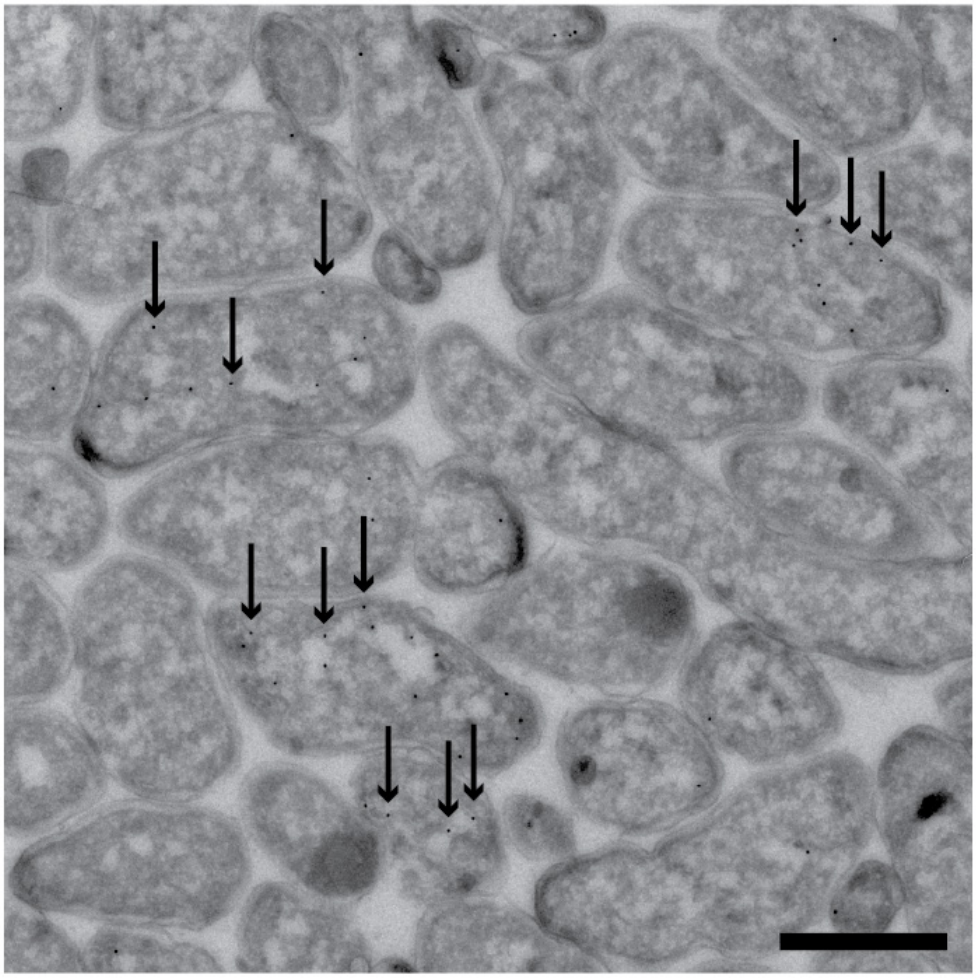

Figure 6: EM image of azido-*E. coli* mixed 1:25 with Met-treated *E. coli*. After mixing, cells were fixed with 2% PFA and subjected to Tokuyasu sample preparation (including gelatin embedding and sucrose infiltration) prior to cryosectioning into 75 nm sections. An on-section ccHc reaction was performed to react azido-*E. coli* cells with AlexaFluor-488 alkyne. AlexaFluor-488 was then labelled with 15 nm protein A coated gold particles using an anti-AlexaFluor-488 antibody. Arrows indicate gold particles. Scale bar 1 µm.

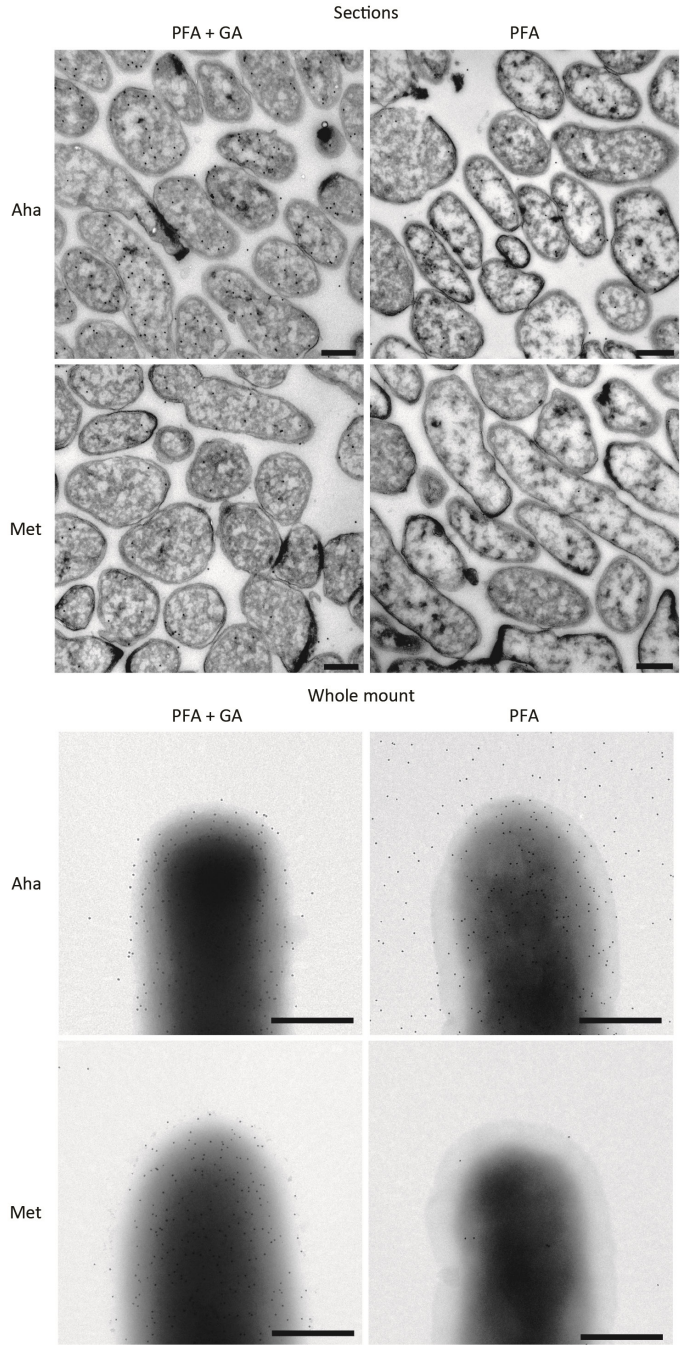

Figure 7: Upper panel; Azido-*E. coli* and Met-treated *E. coli* fixed with either 2% PFA or 2% PFA supplemented with 0.2% GA and labelled with bioorthogonal gold labelling strategy. Scale bar 1 µm. Lower panel; bioorthogonal gold surface-labelling of Hbp(Δβ-cleav) expressing *E. coli* B834(DE3) bacteria cultured in the presence of either 4 mM Aha or 4 mM Met and fixed with either 2% PFA or 2% PFA supplemented with 0.2% GA. Scale bars 500 nm.

It was then verified whether bioorthogonal labels could be additionally detected in an EM setting using a CLEM approach. To this end a strategy was developed that is outlined in Figure 8A. Mixed azido-*E. coli* and Met-incubated *E. coli* were cryosectioned and transferred to a TetraSpeck bead-containing EM grid and were labelled with AlexaFluor-488-alkyne using a ccHc-reaction. These sections were then imaged with the confocal microscope and were embedded in methyl cellulose with uranyl acetate and subjected to EM imaging. Correlation of the confocal- and EM-images was performed using TetraSpeck beads[37] as fiducials (Figure 8A and 9). Results show that CLEM imaging of azides using bioorthogonal labelling is selective and that the ccHc reaction has sufficient signal-to-noise ratio for the detection of fluorescently-labelled azides in ultrathin sections (Figure 8B).

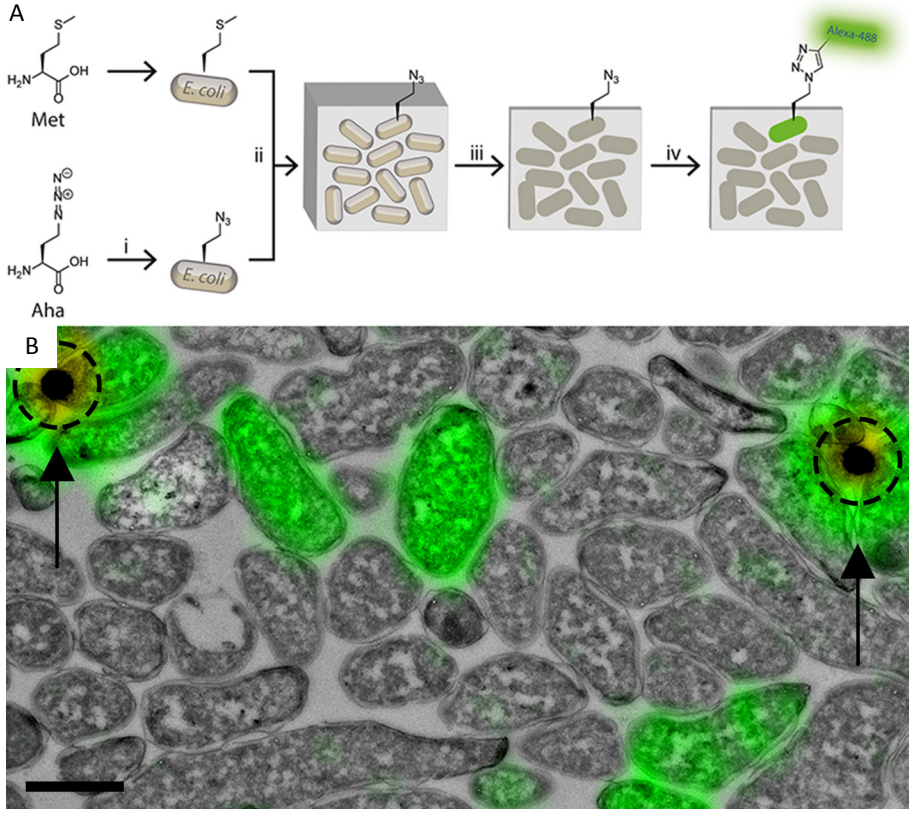

Figure 8: A) Schematic overview of bioorthogonal labelling strategy for CLEM-imaging. Azido and unlabelled *E. coli* were mixed in non-equal ratio (1:25). After Tokuyasu sample preparation and cryosectioning into 75 nm sections, a ccHc-reaction with AlexaFluor-488 was performed. B) CLEM-image of the above experiment. Green: AlexaFluor-488 label. Dotted circles: signal from the 100 nm TetraSpeck beads. Scale bar 1 µM.

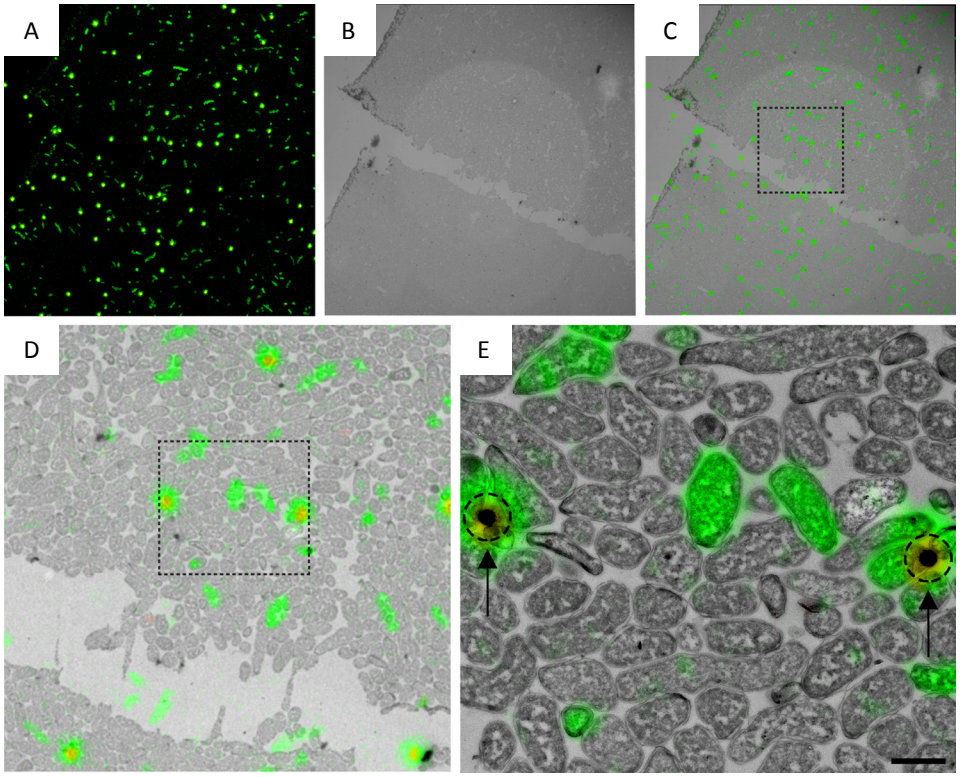

Figure 9: CLEM image of azido-*E. coli* B834(DE3) in a mixture with unlabelled *E. coli* B834(DE3) (A) Confocal microscopy image of azido-*E. coli* B834(DE3) in a mixture with unlabelled *E. coli* B834(DE3). Green: AlexaFluor-488 and 100 nm TetraSpeck beads, Yellow = 100 nm Tetraspeck bead. (B) EM image of azido-*E. coli* B834(DE3) in a mixture with unlabelled *E. coli* B834(DE3). (C) CLEM image obtained from figure A and B using section shape for correlation. (D) Detail from C. Green: AlexaFluor-488 alkyne and 100 nm TetraSpeck beads, Yellow 100 nm Tetraspeck beads. Tetraspeck beads were used for correlation. (E) Detail from D. Green: AlexaFluor-488 alkyne and 100 nm TetraSpeck beads, Yellow 100 nm Tetraspeck beads (indicated with circles and arrows). Tetraspeck beads were used for correlation. Scale bar 1 μM.

Conclusion

Two methods were developed for the EM detection of intracellular bioorthogonal groups on ultrathin cryosections. The first method is a bioorthogonal gold labelling strategy that allows for the direct detection of gold-labelled bioorthogonal tags in the EM. The second method uses CLEM for the detection of bioorthogonal labels in cryosectioned biological samples. This approach provides facile detection of bioorthogonal tags with fluorescence microscopy and gives ultrastructural information on the cellular location of these tags using EM. Both methods show that bioorthogonal labelling can be used to

selectively label and localise the presence of bioorthogonal tags with EM in a non-homogenous sample of tagged and untagged *E. coli*.

Since a wide variety of both templated and non-templated biomolecules can be modified by this method, it is foreseen that these labelling stratagies can be applied to address a wide range of research questions, which would benefit from the combination of these bioorthogonal labels and the ultrastructural context provided by EM. A final advantage and challenge would be to image biomolecules in organisms for which genetic modification is not an option, such as many bacterial and viral pathogens, which could lead to new insights regarding infectivity and clearance of these organisms by host cells. Furthermore, the stability of azides[38] to intracellular conditions would allow imaging of events long after the degradation of reporter proteins.

Experimental

E. coli culturing conditions and growth measurements

E. coli B834(DE3) bacteria were grown overnight at 37°C in Lysogeny Broth (LB) medium. The following day cultures were diluted 1:50 in LB medium and grown at 37°C untill an OD_{600} between 0.3-0.5 was reached. Subsequently cells were collected and resuspended in Selenomet medium (Molecular Dimensions) and supplemented with different concentrations of either Aha (Bachem) or Met (Sigma-Aldrich). After 30 minutes, 1 h, 2 h and 3 h OD_{600} were measured and cells were collected by centrifugation (13,000 x g for 1 minute) for further analysis. To monitor the outgrowth of *E. coli* cells that were cultured in the presence of Aha/Met, cells were collected by centrifugation (13,000 x g for 1 minute) at the indicated time points, after which Aha/Met-containing medium was replaced for LB medium and OD_{600} measurements were performed.

E. coli B834(DE3)Hbp(Δβ-cleav) bacteria were grown overnight at 37°C in LB medium supplemented with chloramphenicol (cam) (f.c. 30 µg/ml). The following day cultures were diluted 1:50 in LB medium with cam (f.c. 30 µg/ml) and grown at 37°C untill an OD_{600} between 0.3-0.5 was reached. Subsequently cells were collected and resuspended in Selenomet medium (Molecular Dimensions) and supplemented with either 4 mM Aha (Bachem) or 4 mM Met (Sigma-Aldrich). Expression of HbpΔβ-cleav was induced by addition of 1 mM Isopropyl β-D-1-thiogalactopyranoside (IPTG, Sigma-Aldrich). After 2 h of induction cells were collected by centrifugation (13,000 x g for 1 minute) for further analysis.

Inclusion body analysis

At the indicated time points *E. coli* cells were fixed for 2 h with 2% PFA in 0.1 M phosphate buffer. The fixed cells were harvested by centrifugation (13,000 x g for 1 minute) and resuspended in PBS. Formvar carbon-coated copper grids were floated on small drops of fixed *E. coli* cells for 5 minutes at room temperature. Grids were then washed on 3 drops of PBS and 10 drops of aquadest. Cells were imaged with a Tecnai 12 transmission electron microscope (FEI) at 120 kV acceleration voltage.

SDS-PAGE Analysis

At the indicated time points *E. coli* B834(DE3) cells were collected and lysed with lysis buffer (50 mM HEPES pH 7.3, 150 mM NaCl and 1% NP-40) and incubated on

ice for 1 h. Subsequently protein concentrations were determined with a Quibit 2.0 fluorimeter (Life Technologies), after which 20 µg of the protein was incubated for 1 h with ccHc-cocktail (0.1 M HEPES pH 7.3, 1 mM $CuSO_4$, 10 mM sodium ascorbate, 1 mM THPTA ligand, 10 mM amino-guanidine, 5 µM AlexaFluor-488 alkyne (Invitrogen)). Samples were then resuspended in 4x SDS Sample buffer (250 mM Tris.HCl pH 6.8, 8% w/v SDS, 40% glycerol, 0.04% w/v bromophenol blue, 5% 2-mercaptoethanol) and incubated at 100°C for 5 minutes. After the samples were run through a Hamilton syringe multiple times to shear genomic DNA, samples were subjected to SDS-PAGE. Gels were then directly imaged with a Biorad Universal Hood III for in-gel visualisation of fluorescent labelling. As a loading control gels were stained with Coomassie Brilliant Blue. PageRuler Plus Prestained Protein Ladder (Thermo Scientific) was used as a protein standard.

At the indicated time points *E. coli* B834(DE3)Hbp(Δβ-cleav) cells were collected and lysed with lysis buffer (50 mM HEPES pH 7.3, 150 mM NaCL and 1% NP-40) and incubated on ice for 1 h. Subsequently protein concentrations were determined with a Quibit 2.0 fluorimeter (Life Technologies). Samples were then resuspended in 4x SDS Sample buffer (250 mM Tris.HCl pH 6.8, 8% w/v SDS, 40% glycerol, 0.04% w/v bromophenol blue, 5% 2-mercaptoethanol) and incubated at 100°C for 5 minutes. After the samples were run through a Hamilton syringe multiple times to shear genomic DNA, samples were subjected to SDS-PAGE. Approximately 20 µg protein was loaded per lane. Gels were then stained with Coomassie Brilliant Blue. PageRuler Plus Prestained Protein Ladder (Thermo Scientific) was used as a protein standard.

Bioorthogonal gold labelling on whole mount E. coli B834(DE3)
At the indicated time points *E. coli* B834(DE3)wt and *E. coli* B834(DE3)HbpΔβ-cleav cells were collected and resuspended in either 4% PFA in 0.1 M phosphate buffer or 4% PFA, 0.2% GA in 0.1 M phosphate buffer for 1 h at room temperature. The fixed cells were harvested by centrifugation (13,000 x g for 1 minute), resuspended in storage solution (0.5% PFA in 0.1 M phosphate buffer) and kept at 4°C until further analysis.

Fixed *E. coli* cell pellets, containing ~1 OD_{600} were resuspended in blocking buffer (1% Bovine Serum Albumin (BSA), 1% Gelatin from Cold Water Fish (GCWSF) in 0.1

M HEPES pH 7.3) and blocked for 15 minutes. Subsequently cells were collected by centrifugation (13,000 x g for 1 minute) and resuspended in click cocktail (0.1 M HEPES pH 7.3, 1 mM $CuSO_4$, 10 mM sodium ascorbate, 1 mM THPTA ligand, 10 mM amino-guanidine, 5 µM AlexaFluor-488 alkyne (Invitrogen)). The cells were incubated for 1 h with the click cocktail, then washed 3 times with HEPES 0.1 M pH 7.3. Subsequently Formvar carbon-coated copper grids were floated on small drops of the fluorescently-click-labelled *E. coli* cells for 5 minutes at room temperature. Grids were then washed on 3 drops of PBS and blocked with 1% BSA in PBS for 15 minutes. Next, the grids were incubated for 1 h with an AlexaFluor-488 antibody diluted in PBS supplemented with 1% BSA. After 5 washes with PBS, the antibodies were probed with protein A conjugated to 15 nm gold (PAG; CMC, Utrecht University). Labellings were imaged with an Tecnai 12 transmission electron microscope (FEI) at 120 kV acceleration voltage.

Preparation of cryosections

Samples were prepared for cryosectioning as described elsewhere.[39] Briefly, *E. coli* cells were fixed for 24 h in freshly prepared 2% PFA in 0.1 M phosphate buffer with or without 0.2% GA. Fixed cells were embedded in 12% gelatin (type A, bloom 300, Sigma Aldrich) and cut with a razor blade into 0.5 mm^3 cubes. The sample blocks were infiltrated in phosphate buffer containing 2.3 M sucrose for 3 h. Sucrose-infiltrated sample blocks were mounted on aluminium pins and plunged in liquid nitrogen. The frozen samples were stored under liquid nitrogen.

Ultrathin *E.coli* cell sections of 75 nm were obtained as described elsewhere.[39] Briefly, the frozen sample was mounted in a cryo-ultramicrotome (Leica). The sample was trimmed to yield a squared block with a front face of about 300 x 250 µm (Diatome trimming tool). Using a diamond knife (Diatome) and antistatic devise (Leica) a ribbon of 75 nm thick sections was produced that was retrieved from the cryo-chamber with a droplet of 1.15 M sucrose containing 1% methylcellulose. Obtained sections were transferred to a specimen grid previously coated with formvar and carbon. In case of CLEM imaging, grids were additionally coated as indicated with 100 nm TetraSpeck beads (Life Technologies).

Bioorthogonal gold labelling on cryosections

Sections were labelled as follows: thawed cryosections on an EM grid were left for 30 minutes on the surface of 2% gelatin in phosphate buffer at 37°C. Subsequently,

grids were incubated on drops of PBS/glycine and PBS/glycine containing 1% BSA. Grids were then incubated on top of the ccHc- cocktail (0.1 M HEPES pH 7.3, 1 mM $CuSO_4$, 10 mM sodium ascorbate, 1 mM THPTA ligand, 10 mM amino-guanidine, 5 µM AlexaFluor-488 alkyne (Invitrogen) for 1 h and washed 6 times with PBS. Then the grids were blocked again with PBS/glycine containing 1% BSA after which the grids were incubated for 1 h with PBS/glycine 1% BSA supplemented with an AlexaFluor-488 antibody (Invitrogen). After washing with PBS/glycine and blocking with PBS/glycine 0.1% BSA, grids were incubated for 20 minutes on PBS/glycine 1% BSA supplemented with 15 nm PAG (CMC, Utrecht University). Grids were then washed with PBS, and washed 10 times with aquadest, after which they were incubated for 5 minutes on droplets of uranylacetate/methylcellulose. Excessive uranylacetate/methylcellulose was blotted away and grids were dried to air. Labellings were imaged with a Tecnai 12 Biotwin transmission electron microscope (FEI) at 120 kV acceleration voltage.

Bioorthogonal fluorophore labelling on cryosections

Sections were labelled as follows: thawed cryosections on an EM grid were left for 30 minutes on the surface of 2% gelatin in phosphate buffer at 37°C. Subsequently grids were incubated on drops of PBS/glycine and PBS/glycine containing 1% BSA. Grids were then incubated on top of the ccHc-cocktail (0.1 M HEPES pH 7.3, 1 mM $CuSO_4$, 10 mM sodium ascorbate, 1 mM THPTA ligand, 10 mM amino-guanidine, 5 µM AlexaFluor-488 alkyne (Invitrogen) for 1 h and washed 6 times with PBS and 10 times with aquadest.

Microscopy and correlation

The CLEM approach used was adapted from Vicidomini et al.[21] Grids containing the sample sections were washed with 50% glycerol and placed on glass slides (pre- cleaned with 100% ethanol). Grids were then covered with a small drop of 50% glycerol after which a coverslip was mounted over the grid. Coverslips were fixed using Scotch Pressure Sensitive Tape. Samples were imaged with a Leica TCS SP8 confocal microscope (63x oil lens, N.A.=1.4). Confocal microscopy was used as it allowed to make image stacks from the sections at different focus planes; this was convenient as the sections were found to be in different focus planes whilst placed between the glass slides and coverslip. After fluorescence microscopy the EM grid with the sections was remove from the glass slide, rinsed in distilled water and incubated for 5 minutes on droplets of uranylacetate/methylcellulose.

Excess of uranylacetate/methylcellulose was blotted away and grids were air-dried. EM imaging was performed with a Tecnai 12 Biotwin transmission electron microscope (FEI) at 120 kV acceleration voltage.

Correlation of confocal and EM images was performed in Photoshop CS6. In Adobe Photoshop, the LM image was copied as a layer into the EM image and made 50% transparent. Transformation of the LM image was necessary to match it to the larger scale of the EM image. This was performed via isotropic scaling and rotation. Interpolation settings; bicubic smoother. Alignment at high magnification was carried out using fiducial beads.[40]

References

1. H. C. Kolb, M. G. Finn and K. B. Sharpless, *Angew Chem Int Ed Engl*, 2001, **40**, 2004-2021.
2. E. M. Sletten and C. R. Bertozzi, *Angew Chem Int Ed Engl*, 2009, **48**, 6974-6998.
3. C. P. Ramil and Q. Lin, *Chem Commun (Camb)*, 2013, **49**, 11007-11022.
4. E. Saxon and C. R. Bertozzi, *Science*, 2000, **287**, 2007-2010.
5. S. Ito, L. Shen, Q. Dai, S. C. Wu, L. B. Collins, J. A. Swenberg, C. He and Y. Zhang, *Science*, 2011, **333**, 1300-1303.
6. A. J. Perez and H. B. Bode, *J Lipid Res*, 2014, **55**, 1897-1901.
7. M. S. Siegrist, S. Whiteside, J. C. Jewett, A. Aditham, F. Cava and C. R. Bertozzi, *ACS Chem Biol*, 2013, **8**, 500-505.
8. G. W. Liechti, E. Kuru, E. Hall, A. Kalinda, Y. V. Brun, M. VanNieuwenhze and A. T. Maurelli, *Nature*, 2014, **506**, 507-510.
9. A. E. Speers, G. C. Adam and B. F. Cravatt, *J Am Chem Soc*, 2003, **125**, 4686-4687.
10. H. Ovaa, P. F. van Swieten, B. M. Kessler, M. A. Leeuwenburgh, E. Fiebiger, A. M. van den Nieuwendijk, P. J. Galardy, G. A. van der Marel, H. L. Ploegh and H. S. Overkleeft, *Angew Chem Int Ed Engl*, 2003, **42**, 3626-3629.
11. E. M. Sletten and C. R. Bertozzi, *Acc Chem Res*, 2011, **44**, 666-676.
12. R. S. Erdmann, H. Takakura, A. D. Thompson, F. Rivera-Molina, E. S. Allgeyer, J. Bewersdorf, D. Toomre and A. Schepartz, *Angew Chem Int Ed Engl*, 2014, **53**, 10242-10246.
13. D. W. Dorward, *Methods Mol Biol*, 2008, **431**, 173-187.
14. J. Roth, *Histochem Cell Biol*, 1996, **106**, 1-8.
15. G. Griffiths, in *Fine Structure Immunocytochemistry*, Springer Berlin Heidelberg, Berlin, Heidelberg, 1993, DOI: 10.1007/978-3-642-77095-1_2, pp. 9-25.
16. T. M. Mayhew and J. M. Lucocq, *Histochem Cell Biol*, 2008, **130**, 299-313.
17. K. A. Sjollema, U. Schnell, J. Kuipers, R. Kalicharan and B. N. Giepmans, *Methods Cell Biol*, 2012, **111**, 157-173.
18. B. N. Giepmans, *Histochem Cell Biol*, 2008, **130**, 211-217.
19. E. Bos, L. Hussaarts, J. R. van Weering, M. H. Ellisman, H. de Wit and A. J. Koster, *J Struct Biol*, 2014, **186**, 273-282.
20. G. Vicidomini, M. C. Gagliani, M. Canfora, K. Cortese, F. Frosi, C. Santangelo, P. P. Di Fiore, P. Boccacci, A. Diaspro and C. Tacchetti, *Traffic*, 2008, **9**, 1828-1838.
21. G. Vicidomini, M. C. Gagliani, K. Cortese, J. Krieger, P. Buescher, P. Bianchini, P. Boccacci, C. Tacchetti and A. Diaspro, *Microsc Res Tech*, 2010, **73**, 215-224.

22. M. Grabenbauer, *Methods Cell Biol*, 2012, **111**, 117-138.
23. J. H. Luft, *J Biophys Biochem Cytol*, 1961, **9**, 409-414.
24. J. W. Slot and H. J. Geuze, *Nat Protoc*, 2007, **2**, 2480-2491.
25. K. L. Kiick, E. Saxon, D. A. Tirrell and C. R. Bertozzi, *Proc Natl Acad Sci U S A*, 2002, **99**, 19-24.
26. K. L. Kiick, J. C. M. van Hest and D. A. Tirrell, *Angew Chem Int Ed Engl*, 2000, **39**, 2148-2152.
27. D. J. Leahy, W. A. Hendrickson, I. Aukhil and H. P. Erickson, *Science*, 1992, **258**, 987-991.
28. W. B. Wood, *J Mol Biol*, 1966, **16**, 118-133.
29. A. K. Upadhyay, A. Murmu, A. Singh and A. K. Panda, *PLoS One*, 2012, **7**, e33951.
30. R. Hatzenpichler, S. Scheller, P. L. Tavormina, B. M. Babin, D. A. Tirrell and V. J. Orphan, *Environ Microbiol*, 2014, **16**, 2568-2590.
31. Z. P. Demko and K. B. Sharpless, *Angew Chem Int Ed Engl*, 2002, **41**, 2113-2116.
32. C. W. Tornoe, C. Christensen and M. Meldal, *J Org Chem*, 2002, **67**, 3057-3064.
33. Q. Wang, T. R. Chan, R. Hilgraf, V. V. Fokin, K. B. Sharpless and M. G. Finn, *J Am Chem Soc*, 2003, **125**, 3192-3193.
34. W. S. P. Jong, C. M. Ten Hagen-Jongman, T. Den Blaauwen, D. Jan Slotboom, J. R. H. Tame, D. Wickström, J.-W. De Gier, B. R. Otto and J. Luirink, *Molecular Microbiology*, 2007, **63**, 1524-1536.
35. W. S. P. Jong, M. H. Daleke-Schermerhorn, D. Vikström, C. M. ten Hagen-Jongman, K. de Punder, N. N. van der Wel, C. E. van de Sandt, G. F. Rimmelzwaan, F. Follmann, E. M. Agger, P. Andersen, J.-W. de Gier and J. Luirink, *Microbial Cell Factories*, 2014, **13**, 162.
36. K. T. Tokuyasu, *J Cell Biol*, 1973, **57**, 551-565.
37. W. Kukulski, M. Schorb, S. Welsch, A. Picco, M. Kaksonen and J. A. Briggs, *J Cell Biol*, 2011, **192**, 111-119.
38. J. B. Pawlak, G. P. Gential, T. J. Ruckwardt, J. S. Bremmers, N. J. Meeuwenoord, F. A. Ossendorp, H. S. Overkleeft, D. V. Filippov and S. I. van Kasteren, *Angew Chem Int Ed Engl*, 2015, **54**, 5628-5631.
39. P. J. Peters, in *Current Protocols in Cell Biology*, John Wiley & Sons, Inc., 2001.
40. J. Kuipers, T. J. van Ham, R. D. Kalicharan, A. Veenstra-Algra, K. A. Sjollema, F. Dijk, U. Schnell and B. N. Giepmans, *Cell Tissue Res*, 2015, **360**, 61-70.